Environmental Science
Processes & Impacts

Comparing Photodegradation Model Systems: Measuring Bimolecular Rate Constants Between Photochemically Produced Reactive Intermediates and Organic Contaminants

Journal:	*Environmental Science: Processes & Impacts*
Manuscript ID	EM-ART-03-2025-000199.R1
Article Type:	Paper

Comparing Photodegradation Model Systems: Measuring Bimolecular Rate Constants Between Photochemically Produced Reactive Intermediates and Organic Contaminants

Luana de Brito Anton,[1] Andrea I. Silverman,[1] and Jennifer N. Apell[1*]

[1]Civil and Urban Engineering Department, Tandon School of Engineering, New York University, Brooklyn, New York 11201, United States

*Corresponding author: japell@nyu.edu

ABSTRACT

Predicting the environmental fate of anthropogenic chemicals remains a top priority for scientists and regulators; however, these efforts are hindered by the complexity of environmental systems. For example, in aquatic photodegradation, multiple photochemically produced reactive intermediates (PPRI) are present simultaneously, such as hydroxyl radicals (•OH), singlet oxygen ($^1O_2$), and triplet excited states of chromophoric dissolved organic matter (^{3}CDOM*). This makes it difficult to isolate contributions of individual PPRI to overall photodegradation as well as measure bimolecular reaction rate constant with target contaminants (k_{PPRI}), which could subsequently be used to predict degradation rates under variable environmental conditions and in engineered treatment systems. As an alternative approach, simplified model systems can be used to isolate reactions with each PPRI. Yet, a systematic comparison of the results obtained in different model systems has not been conducted. In this study, at least two model systems were used to quantify k_{PPRI} between each PPRI (i.e., •OH, $^1O_2$, and three ^{3}CDOM* proxies) and each of the 28 pesticides evaluated. Results were consistent for most pesticides across the set of model systems used to evaluate a given PPRI. However, significant discrepancies were observed in some

cases. For some pesticides, reactions with •OH appeared faster than the diffusion-controlled limit, suggesting additional reactions with unidentified PPRI were occurring. In $^1O_2$ model systems, unexpected reactions occurred between some pesticides and the triplet excited state of the model sensitizer. Lastly, there was not a consistent trend between the calculated k_{PPRI} and the photochemical properties of the three ^{3}CDOM* proxies evaluated as suggested in previous studies. Overall, the results from this study showed that model systems are a powerful tool for investigating indirect photodegradation reactions and should be adopted in formal evaluations of the environmental fate of anthropogenic chemicals. Key considerations and recommendations to ensure accurate and reliable use of model systems are provided and areas benefiting from further investigation are identified.

ENVIRONMENTAL SIGNIFICANCE

Bimolecular reaction rate constants between photochemically produced reactive intermediates (PPRI) and organic contaminants are needed to predict their fate in sunlit waters. Model systems are a valuable tool for investigating specific PPRI reactions compared to irradiating natural waters. This study measured and compared bimolecular reaction rate constants between 28 pesticides and PPRI, specifically hydroxyl radicals, singlet oxygen, and triplet excited states of organic molecules. This systematic investigation showed comparable results across model systems for a given PPRI in most cases, but occasional differences highlight the importance of control experiments and the potential for unexpected and confounding reactions. Recommended experimental procedures and control experiments are provided based on the results.

INTRODUCTION

Environmental contaminants can be degraded by reactions with photochemically produced reactive intermediates (PPRI) that are generated when naturally occurring chromophoric dissolved organic matter (CDOM) absorbs sunlight.[1, 2] Among the various PPRI produced in sunlit waters, hydroxyl radicals (•OH), singlet oxygen ($^1O_2$), and triplet excited states of CDOM (^{3}CDOM*) were previously found to have significant reaction rates with many anthropogenic chemicals, including pesticides[1, 2] and pharmaceuticals.[3, 4] Among these anthropogenic chemicals, only pesticides are regularly evaluated for the potential to undergo photodegradation because of regulations like the United States (US) Federal Insecticide, Fungicide, and Rodenticide Act.

The US Environmental Protection Agency (EPA) created guidelines[5] for studying the indirect photodegradation of pesticides, which recommends using a synthetic water prepared using commercially available organic matter isolates. This approach, however, generates multiple PPRI simultaneously and makes it difficult to identify reaction mechanisms and quantify bimolecular reaction rate constants between PPRI and target compounds (k_{PPRI}) that are needed to predict degradation under varying environmental conditions. As an alternative, simplified model systems, which include only the well-studied chemicals necessary, can be used to isolate specific reaction pathways and quantify k_{PPRI}.

In this work, model systems are defined as the combination of (1) the sensitizer used to selectively produce a specific PPRI, (2) the probe compound (i.e., a compound with a known bimolecular reaction rate constant with the PPRI) used to measure the PPRI steady-state concentration, and (3) the experimental solution, which could include buffers or chemicals that quench or extend the lifetime of specific PPRI. By measuring and comparing the degradation rates of target and probe compounds, k_{PPRI} can be calculated through competition kinetics. Many

combinations of model sensitizers and probe compounds have been previously used to investigate the reactivity of PPRI with organic contaminants (see Tables 2.1, 3.1, and 4.1 for examples). Yet, the comparability and robustness of different model systems has not been systematically evaluated for a diverse range of compounds. While either the sensitizer, probe compound, or solution composition can be changed to create different model systems, the model systems used in this work primarily focused on using different sensitizers.

Accurate measurements of k_{PPRI} are needed for improving predictions of environmental fate of chemicals and exposure pathways. Recently, environmental chemists and toxicologists in North America identified the ability to better predict the fate of chemical pesticides in the environment as a top research priority to attain sustainable agriculture practices.[6] Therefore, 28 pesticides with a range of chemical structures were chosen for investigation in this study. Pesticides were selected for inclusion in this study if the pesticide registration dossier[7] reported photolysis and/or water phase half-lives that were relatively short ($t_{1/2}$<60 days) and negligible hydrolysis. Discrepancies across model systems were identified, and recommendations and key considerations for optimal experimental procedures are provided. Finally, the significance of reactions with PPRI for the environmental fate of the pesticides investigated was evaluated based on the k_{PPRI} measured.

MATERIALS AND METHODS

Materials

All 28 pesticides were Pestanal grade with ≥95% purity (Table S1.1). Model sensitizers included hydrogen peroxide (H_2O_2, 30% unstabilized) and sodium nitrite ($NaNO_2$) to generate •OH, which were chosen because they are commonly used and have well-known reaction

mechanisms.[1, 8, 9] For $^1O_2$ model systems, zinc porphyrin (ZnP, Zn 5,10,15,20-tetra-(4-pyridyl)-21H,23H-porphine tetrakis-(methochloride)) and perinaphthenone (PN) were the chosen sensitizers because of their lower one-electron reduction potentials and triplet excited state energies compared to ^{3}CDOM* and because their $^1O_2$ quantum yields are close to unity.[10, 11] Therefore, in the $^1O_2$ model systems, reactions between target compounds and the triplet excited states of the sensitizer were expected to be negligible compared to reactions with $^1O_2$. Three sensitizers were chosen as ^{3}CDOM* proxies; benzophenone (BP), 4-carboxybenzophone (4-CBBP), and 3-methoxyacetophenone (3-MAP) were previously reported to have triplet excited state photochemical properties within the range measured for natural CDOM mixtures and have been suggested for use in previous studies.[11-14] While using sensitizers that are simple molecules eliminate possibly confounding reaction pathways compared to irradiating natural CDOM solutions, the production of $^1O_2$ from the triple excited state of CDOM or sensitizers inextricably link these two PPRI. To further differentiate between these two reaction pathways, deuterium oxide (D_2O) substituted one of the $^1O_2$ model systems at an 80:20 D_2O:H_2O volume ratio to quantify the kinetic solvent isotope effect.[15]

Further solution components included either benzoic acid, furfuryl alcohol (FFA), or 2,4,6-trimethylphenol (TMP) as probe compounds to quantify •OH, $^1O_2$, and triplet excited states of the sensitizer (^{3}sens*), respectively. Phenol was used as a model antioxidant in ^{3}sens* model systems. All stock solutions were prepared in HPLC-grade acetonitrile or ultrapure water (≥18.2 MΩ, Millipore Direct-Q 3 UV), whereas working solutions were prepared in 1 mM phosphate buffer at pH=7 except for prothioconazole. Prothioconazole has an environmentally relevant pKa of 7.3 (Text S1.2, Figure S1.1), and experimental solutions were prepared at pH=5 and pH=9, both using 1 mM phosphate buffers. Given the use of competition kinetics to calculate k_{PPRI}, the presence of

≤0.1% v/v acetonitrile as a co-solvent did not impact the results (Text S2.1). In a separate test tube, p-nitroanisole (PNA) solution was used as the actinometer.[16]

More information on chemicals and solution preparation is provided in Text S1.1 and Table S1.1.

Molar Absorptivity

The molar absorptivity of the sensitizers and probe compounds were measured in ultrapure water using a UV-vis spectrophotometer (Cary 60, Agilent). Measurements were taken at a minimum of four concentrations (0.1–20 mg L^{-1}) and included at least seven independent scans using a combination of 1 and 10 cm pathlength quartz cuvettes. The data were combined and fit with a series of Gaussian curves for reconstructing the full molar absorptivity spectrum from the three Gaussian curve parameters (Table S1.2, Figure S1.2).[16]

Experimental Setup and Sample Analysis

Experiments were conducted in a merry-go-round photoreactor (Luzchem LZC-4V)[16] using 8 UVA bulbs (λ_{max}=350 nm) placed on the sides of the photoreactor (Figure S1.3). The air temperature in the photoreactor was 20-25 °C during experiments. The experimental solutions included the pesticide, sensitizer, probe compound, and buffer (Text S1.1) in Pyrex test tubes (10 mm internal diameter, 8 mL of solution). Each experiment had at least three independent replicates performed, and up to seven 180 μL subsamples were collected during the course of each experiment. PNA (10 μM) solutions were added in separate test tubes to measure the photon fluence in all experiments.

Dark controls were performed under all experimental conditions for each pesticide. In $^1O_2$ model systems, control experiments without the addition of the probe compound (FFA) were conducted. In ^{3}sens* model systems, control experiments included sparging the solutions with nitrogen gas to evaluate the possible contribution of $^1O_2$ to pesticide degradation as well as irradiating solutions without the addition of the probe compound (TMP), to evaluate the influence of TMP on observed degradation rates.

Samples were analyzed using high-performance liquid chromatography with a diode array detector (HPLC-DAD, Agilent 1260) and a 3x150 mm 4-μm HPH-C18 column. The eluents, flow rate, detection wavelength, and retention time for each of the compounds are provided in Table S1.3.

Bimolecular Rate Constant Calculation

The bimolecular reaction rate constant between each PPRI and pesticide (k_{PPRI}) was calculated by multiplying the known bimolecular reaction rate constant of the probe compound ($k_{PPRI,probe}$) and the slope of the best fit line, obtained using linear regression, when plotting the log-linear decay of the pesticide against that of the probe (Equation 1). In Equation 1, [pesticide] and [probe] represent the concentration of each, the subscript *t* represents the experimental time points, and the subscript 0 represents the initial concentration.

$$k_{PPRI} = \frac{\ln\left(\frac{[pesticide]_t}{[pesticide]_0}\right)}{\ln\left(\frac{[probe]_t}{[probe]_0}\right)} \times k_{PPRI,probe} \quad (1)$$

Previously determined $k_{PPRI,probe}$ were used for reactions between •OH and benzoate (5.9×10^9 M^{-1} s^{-1}) and $^1O_2$ and FFA (1×10^8 M^{-1} s^{-1} at 22 °C).[17, 18] For each triplet excited state sensitizer,

$k_{^3sens^*,TMP}$ was calculated by comparing the degradation of TMP as a function of the calculated steady-state concentration of ^{3}sens* in solution (Text S1.3, Table S1.4).

Direct photolysis control experiments were conducted by irradiating solutions containing only the pesticide or probe in buffered ultrapure water. Degradation of probe compounds was negligible. For pesticides that underwent direct photolysis under UVA light, k_{PPRI} was calculated using Equation 2.1, where the subscripts *direct* and *indirect* represent the respective contributions of these pathways and $[PPRI]_{ss}$ is the steady-state concentration of the PPRI. Expanding Equation 2.1 in terms of the measured pesticide, probe, and actinometer degradation results in Equation 2.2, where [PNA] is the concentration of the actinometer.

$$k_{PPRI} = \frac{k_{indirect+direct} - k_{direct}}{[PPRI]_{ss}} \quad (2.1)$$

$$k_{PPRI} = \frac{\left[\ln\left(\frac{[pesticide]}{[pesticide]_0}\right)\right]_{indirect+direct} - \left[\ln\left(\frac{[pesticide]}{[pesticide]_0}\right)\right]_{direct}}{\ln\left(\frac{[PNA]}{[PNA]_0}\right)} \times \left[\frac{\ln\left(\frac{[probe]}{[probe]_0}\right)}{\ln\left(\frac{[PNA]}{[PNA]_0}\right)}\right]^{-1} \times k_{PPRI,probe} \quad (2.2)$$

The errors in k_{PPRI} were calculated using error propagation using the standard error of the slope from linear regression and the error in $k_{PPRI,probe}$. Relative percent differences (RPD) in k_{PPRI} determined in different model systems were calculated as the difference between the values divided by their average.

RESULTS AND DISCUSSION

•OH Model Systems: Hydrogen Peroxide (H_2O_2) and Nitrite (NO_2^-)

For 64% (18 out of 28) of the pesticides, calculated bimolecular reaction rate constants with •OH ($k_{•OH}$) were similar in both model systems (RPDs ≤26%) (Figure 1A, Table S2.1). For most of these pesticides (n=14/18), $k_{•OH}$ was within a factor of two of the diffusion-controlled limit ($\approx 1\times10^{10}$ M^{-1} s^{-1}),[18] and the slowest $k_{•OH}$ was 3.0×10^9 M^{-1} s^{-1}. The $k_{•OH}$ for two of the remaining 10

pesticides – aminopyralid and triclopyr – could only be measured with H_2O_2 as the sensitizer. The •OH steady-state concentration produced with NO_2^- was ≈7 times lower than with H_2O_2, and the observed degradation of these two pesticides in NO_2^- model systems matched the observed direct photolysis rates. For the remaining eight pesticides, the $k_{•OH}$ differed by up to 149%. Literature values of $k_{•OH}$ were found for 14 of the 28 pesticides. These reported $k_{•OH}$ differed by up to 177% from the values measured in this work (Figure S2.2A, Table S2.1).

The two pesticides with the highest discrepancies between model systems – chlorothalonil and protonated prothioconazole – had measured $k_{•OH}$ values higher than the diffusion-controlled limit, which suggests additional reactions with unidentified PPRI are occurring. The identity of these reactions is unclear. Prothioconazole contains a nitrogen-sulfur heterocycle that could be a potential reaction site for additional reaction pathways, and deprotonated prothioconazole rapidly degraded with H_2O_2 in dark controls.[19, 20] Chlorothalonil is known to react via energy transfer resulting in photoreduction and the formation of dechlorination products.[21] While a previous study identified dechlorination products in a $Fe(NO_3)_3/H_2O_2$ photochemical experiment, the proposed mechanism proceeded through hydroxylation, which should not lead to a $k_{•OH}$ above the diffusion-controlled limit.[22]

The six pesticides that had RPDs of 31-97% did not have consistently faster $k_{•OH}$ in one model system versus the other. The $k_{•OH}$ was faster in the NO_2^- system for four pesticides and faster in the H_2O_2 system for two pesticides. This also suggests unidentified reactive intermediates in both systems may contribute to the observed degradation rates.

The calculated $k_{•OH}$ for alachlor, cyprodinil, pyraclostrobin, and trifloxystrobin were 1.4 to 1.7 times faster in the NO_2^- system than the H_2O_2 system. It is known that NO_2^- generates reactive nitrogen species (e.g., $•NO_2$) during irradiation, and a previous study showed that primary and

secondary amines are susceptible to nitrite-sensitized phototransformation.[23] Eight of the studied pesticides contain these amine functional groups, but only cyprodinil and protonated prothioconazole exhibited faster degradation in the NO_2^- model system (Figure S2.1). Additionally, bimolecular reaction rate constants with $\bullet NO_2$ typically ranged from 10^2 to 10^4 M^{-1} s^{-1}, which is orders of magnitude lower than those measured with •OH ($>3\times10^9$ M^{-1} s^{-1}).[24] Therefore, reactions with reactive nitrogen species are not suspected to be the cause of the faster reaction rates observed in the model system. It is also interesting to note that cyprodinil and pyrimethanil are very similar structurally, with the only difference being the replacement of a methyl group by a cyclopropyl group, but still showed distinct behavior (Figure S2.1).

The calculated $k_{\bullet OH}$ for atrazine and mesotrione were 1.5 and 2.7 times faster, respectively, in the H_2O_2 model system. Similar to the NO_2^- system, it is known that the irradiation of H_2O_2 forms other reactive species (e.g., $HO_2\bullet/O_2\bullet^-$, pKa=4.8).[25] For example, superoxide radical ($O_2\bullet^-$) was previously reported to react with atrazine in a quenching experiment and could potentially be the cause of the faster $k_{\bullet OH}$ in the H_2O_2 model system.[26] For mesotrione, however, no studies with these reactive species were found in the literature.

Implications

The observed variations in $k_{\bullet OH}$ between the two model systems highlight the need for further standardization and characterization of these systems used to investigate indirect photodegradation by •OH. While most pesticides had similar values of $k_{\bullet OH}$ across the two model systems, some exhibited evidence of reactions with unknown PPRI in both systems. These additional PPRI remain unidentified, and further study is required to confirm the cause for discrepancies observed in this work. Previous attempts to identify and quantify additional PPRI in

these systems have shown it to be challenging.[23, 27-29] Nevertheless, comparing results across model systems can be used to evaluate potential effects of unknown PPRI and verify the measured $k_{\bullet OH}$.

If using one model system only, the H_2O_2 system is recommended over the NO_2^- system. The 2 mM H_2O_2 model system generated sufficient •OH to complete experiments within four hours and to differentiate reactions with •OH when direct photolysis was significant. Notably, stabilizers added to commercial H_2O_2 may interfere with photochemical reactions, while H_2O_2 decomposition over time can also affect the purity and reactivity of stock solutions. Therefore, unstabilized and fresh H_2O_2 should be used for consistent and higher •OH production. The major drawback of the NO_2^- system is that NO_2^- is both the source and a sink for •OH; therefore, steady-state •OH concentrations were not adjustable and required longer experimental times. Benzoic acid (25 μM) was selected as the probe compound for its historical use in photochemical experiments.[27] In this work, benzoic acid showed strong selectivity for •OH in both model systems as demonstrated by the consistent results across experiments (Text S2.1, Figure S2.3). When comparing the measured $k_{\bullet OH}$ in this study to reported literature values, most studies using p-chlorobenzoic acid as the probe compound found similar $k_{\bullet OH}$ (RPDs ≤23%), whereas studies using other probe compounds tended to have greater differences. Therefore, a systematic comparison of commonly used probes could help identify the optimal compound for quantifying •OH in model systems.

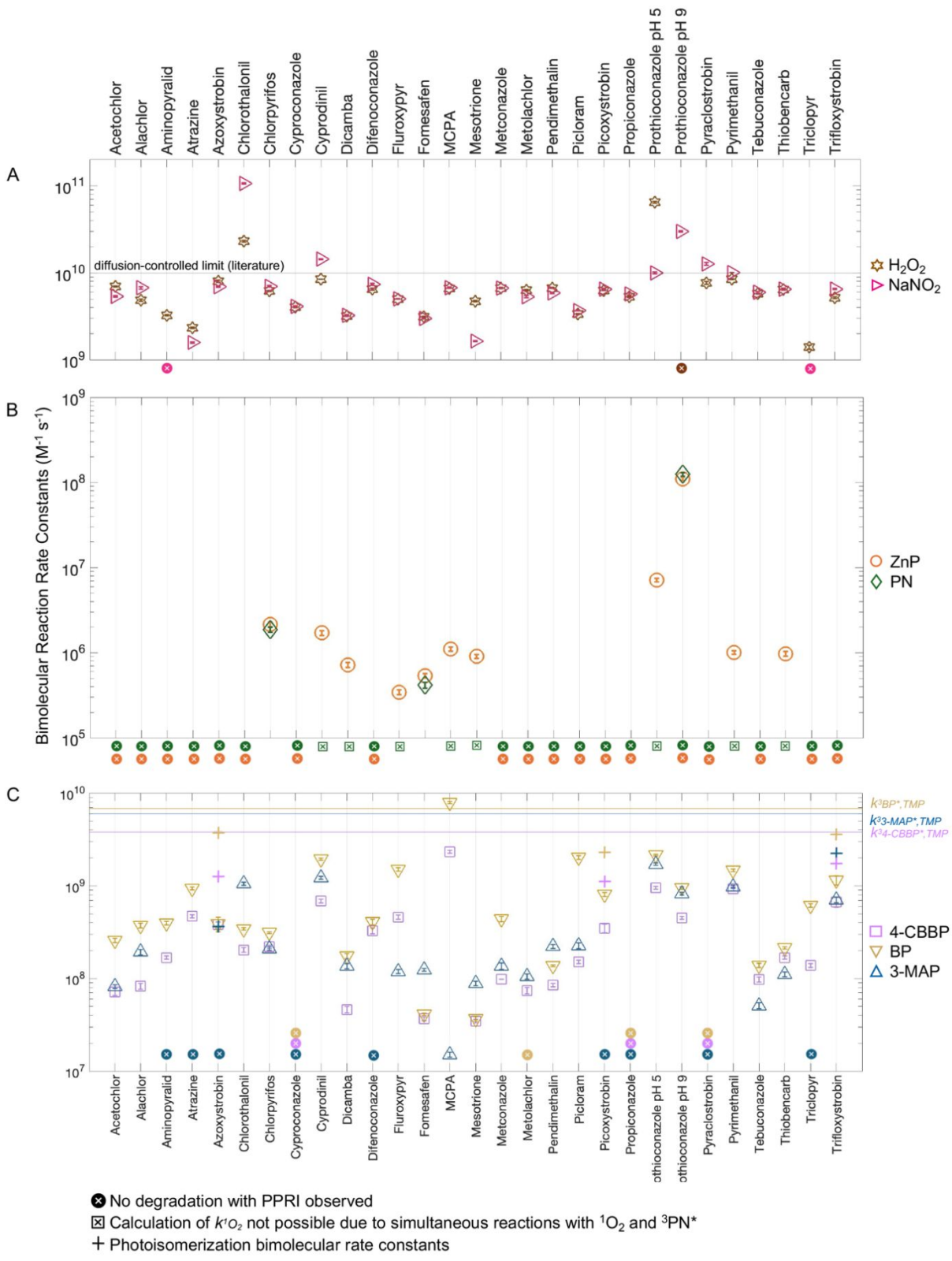
Acetochlor
Alachlor
Aminopyralid
Atrazine
Azoxystrobin
Chlorothalonil
Chlorpyrifos
Cyproconazole
Cyprodinil
Dicamba
Difenoconazole
Fluroxypyr
Fomesafen
MCPA
Mesotrione
Metconazole
Metolachlor
Pendimethalin
Picloram
Picoxystrobin
Propiconazole
Prothioconazole pH 5
Prothioconazole pH 9
Pyraclostrobin
Pyrimethanil
Tebuconazole
Thiobencarb
Triclopyr
Trifloxystrobin
A
diffusion-controlled limit (literature)
H2O2
NaNO2
B
Bimolecular Reaction Rate Constants (M-1 s-1)
ZnP
PN
C
k3BP*,TMP
k3-MAP*,TMP
k3-4-CBBP*,TMP
4-CBBP
BP
3-MAP
No degradation with PPRI observed
Calculation of k1O2 not possible due to simultaneous reactions with 1O2 and 3PN*
Photoisomerization bimolecular rate constants

243

Figure 1. Bimolecular reaction rate constants between the PPRI (•OH, $^1O_2$, and ^{3}sens*) and pesticides (k_{PPRI} in M^{-1} s^{-1}), obtained using (A) H_2O_2 and NO_2^- as model sensitizers to produce •OH, (B) ZnP and PN as model sensitizers to produce $^1O_2$, and (C) 4-CBBP, BP, and 3-MAP as model sensitizers to produce ^{3}sens* (^{3}CDOM* proxies). Pesticide degradation was not observed in some model systems (⊗). Bimolecular reaction rate constants were not calculated when both $^1O_2$ and ^{3}PN* contributed to the observed degradation (☒). Photoisomerization rate constants (+) were measured for three pesticides (i.e., azoxystrobin, picoxystrobin, and trifloxystrobin) in ^{3}sens* model systems. Numerical values of k_{PPRI} are available in Tables S2.1, S3.1, and S4.1.

$^1O_2$ Model Systems: Perinaphthenone (PN), Zinc Porphyrin (ZnP), and D_2O Kinetic Solvent Isotope Effect (KSIE)

Degradation with $^1O_2$ was observed for 36% (10 out of 28) of the pesticides (Figure 1B, Table S3.1). Although chlorothalonil degraded in these systems, no degradation was observed in control experiments without FFA, which could be acting as an electron donor.[21, 30] Observed differences in pesticide degradation in the presence and absence of FFA for the other pesticides were negligible.

Reactions with $^1O_2$ have been previously reported for compounds with sulfide and N-heterocycle groups (e.g., pyrimidine, pyridine).[3, 31, 32] Six of the 10 pesticides that reacted with $^1O_2$ contained these functional groups, but seven of the 18 unreactive pesticides also contained these moieties (e.g., pyridine, pyrimidine, triazine and imidazole rings, Figure S3.1). However, four of the seven unreactive pesticides had significant direct photolysis decay, possibly obscuring slower reactions with $^1O_2$.

Three of the 10 pesticides that degraded in $^1O_2$ systems – chlorpyrifos, fomesafen, and deprotonated prothioconazole – had similar calculated bimolecular reaction rate constants with $^1O_2$ ($k_{^1O_2}$) across model systems (Figure 1B). This can be easily seen when plotting pesticide degradation against FFA degradation, which accounts for differences in $^1O_2$ steady-state concentrations in the PN/H_2O, ZnP/H_2O, and ZnP/D_2O model systems (Figure 2A, Figure S3.2). The consistent slopes indicated that $^1O_2$ was solely responsible for the observed degradation. For the other seven pesticides, the observed degradation rates were slower in the ZnP/D_2O model system, which is observed as a shallower slope when comparing against the other model systems (Figure 2B, Figure S3.2). This indicates that reaction with ^{3}ZnP* or ^{3}PN* was also occurring. Some pesticides (e.g., cyprodinil and pyrimethanil) also had substantially faster (i.e., by ≈80 times) observed degradation in the PN/H_2O model system, indicating that reactions with ^{3}PN* were a dominant degradation pathway (Figure 2C, Figure S3.2). Consequently, the kinetic solvent isotope effect (KSIE) had to be used to calculate the relative contributions of reactions with $^1O_2$ versus ^{3}sens* and determine the $k_{^1O_2}$ for these seven pesticides (Text S3.1).

The presence of D_2O increases the $^1O_2$ steady-state concentrations while not affecting the steady-state concentrations of other reactive intermediates (i.e., ^{3}sens*) or direct photolysis degradation rates (as demonstrated by control experiments).[15] Hence, the fraction of $^1O_2$ reactions ($f_{^1O_2}$) can be calculated by comparing the degradation rates in 80:20 D_2O:H_2O versus H_2O-only systems (Text S3.1).[15] This analysis showed that reactions with $^1O_2$ accounted for 37-59% of the observed degradation for the seven pesticides that reacted with both $^1O_2$ and ^{3}sens* in the ZnP/H_2O model system. The remainder of the observed degradation was attributed to reactions with ^{3}ZnP*. This was unexpected given that the one-electron reduction potential and triplet energy of ZnP are relatively low (Table 1). After correction by $f_{^1O_2}$, $k_{^1O_2}$ were $\leq 5.9\times10^6$ M^{-1} s^{-1} for six of the seven

pesticides (Table S3.1). Deprotonated prothioconazole was the only pesticide that had a $k_{^1O_2}$ that could be environmentally relevant.

Experiments in 80:20 D_2O:H_2O were not conducted with PN as the sensitizer because PN has a higher one-electron reduction potential and triplet energy than ZnP. Therefore, reactions with ^{3}PN* likely occurred in the PN/H_2O model system; consequently, $k_{^1O_2}$ was calculated only for the three pesticides that did not display a KSIE. The $k_{^1O_2}$ calculated for these pesticides were similar (RPDs ≤30%) in all model systems. It would be possible to calculate $k_{^1O_2}$ if results from both a PN/H_2O and PN/D_2O system were available.

Implications

Reactions with ^{3}ZnP* are less likely than with ^{3}PN* due to the lower one-electron reduction potential and triplet energy of ZnP. However, when comparing these two sensitizers, PN (1 μM) is more cost-effective and readily available, making it a practical option for use in model systems. Regardless of the selected sensitizer, D_2O experiments are needed to verify whether ^{3}sens* reactions are occurring and to calculate an accurate $k_{^1O_2}$. Using 80:20 D_2O:H_2O was effective in this study. Higher D_2O volume ratios will result in higher $^1O_2$ steady-state concentrations, but precise control of the D_2O fraction becomes necessary to avoid large errors in calculating $f_{^1O_2}$.[15] FFA (40 μM) has been widely used as a probe compound and has well-studied reaction mechanisms.[27] Nonetheless, control experiments are still needed to account for unexpected reactions – such as the degradation observed for chlorothalonil – that may be caused by the presence of the probe.

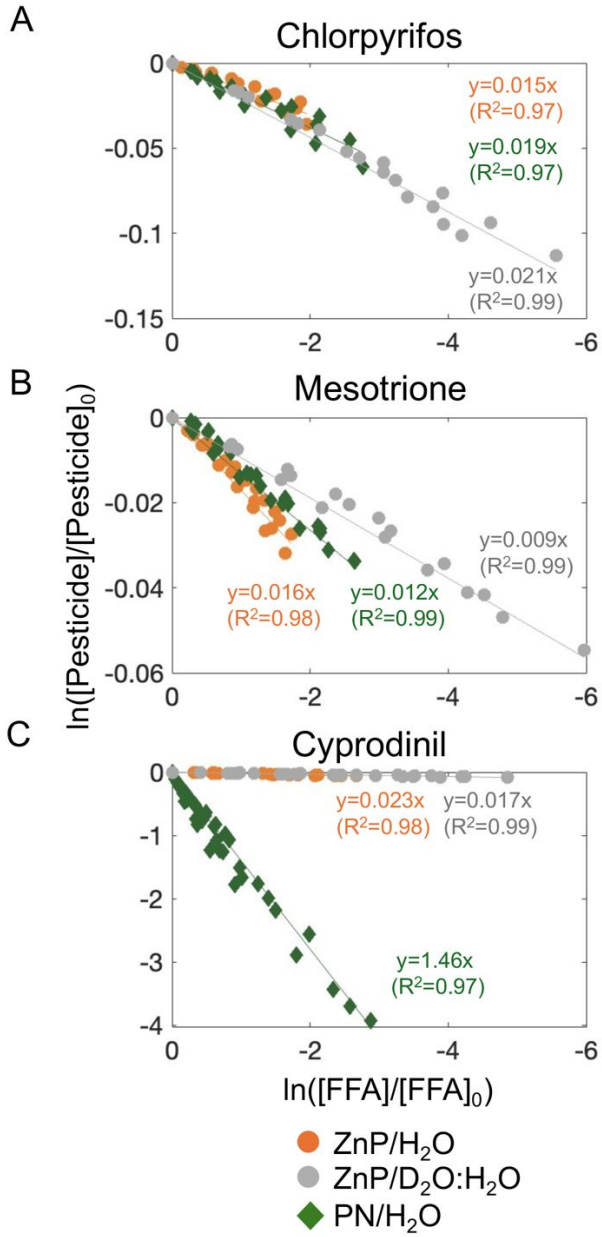

Figure 2. Degradation of pesticides plotted against FFA in ZnP/H_2O, PN/H_2O, and 80:20 D_2O:H_2O/ZnP model systems for (A) chlorpyrifos, (B) mesotrione, and (C) cyprodinil. The slopes of the curves and the coefficient of determination (R^2) are provided. Data for the other pesticides that degraded in $^1O_2$ model systems is shown in Figure S3.2. Bimolecular reaction rate constant values between $^1O_2$ and pesticides ($k_{^1O_2}$) are available in Table S3.1.

Table 1. One-electron reduction potentials ($E^{o*}(^3S^*/S^{-\bullet})$), triplet energies, $^1O_2$ production quantum yields, and bimolecular reaction rate constants with between ^{3}sens* and TMP ($k_{^3sens^*,TMP}$). Calculation of bimolecular reaction rate constants is described in Text S1.3, and the reported uncertainty is calculated from the standard error of the linear regression slope used to calculate $k_{^3sens^*,TMP}$.

Sensitizer	$E^{o*}(^3S^*/S^{-\bullet})$ (V_{SHE})	Triplet Energy (kJ mol^{-1})	$^1O_2$ Quantum Yield	Bimolecular Rate Constant with TMP ($k_{^3sens^*,TMP}$, M^{-1} s^{-1})	
				Literature	This work (Calculated)
Zinc porphyrin complex (ZnP)	0.78 [11]	155 [11]	0.88 [11]	-	-
Perinaphthenone (PN)	1.03 [11]	164 [11]	0.98 [11]	-	-
4-carboxybenzophenone (4-CBBP)	1.83 [33]	286 [33]	-	1.26×10^9 (pH=10.2)[34]	$(3.81 \pm 0.12) \times 10^9$ (pH=7)
Benzophenone (BP)	1.67 [35, 36] 1.79 [37] 1.95 [12, 33]	288 [35, 37]	0.37 [11]	$(5.10 \pm 0.90) \times 10^9$ (pH=8)[38]	$(6.84 \pm 0.14) \times 10^9$ (pH=7)
3-Methoxyacetophenone (3-MAP)	1.64 [36] 1.71 [37]	303 [36, 37]	0.27 [11]	$(2.60 \pm 0.3) \times 10^9$ (pH=8)[38]	$(5.99 \pm 0.11) \times 10^9$ (pH=7)

^{3}CDOM* Model Systems: benzophenone (BP), 4-carboxybenzophenone (4-CBBP), and 3-methoxyacetophenone (3-MAP)

Bimolecular Reaction Rate Constants between Triplet Excited States of Sensitizers (^{3}sens) and TMP*

To quantify bimolecular reaction rate constants between the triplet excited states of the sensitizers (^{3}sens*) and pesticides, the reaction rate constant between the ^{3}sens* and TMP as the probe compound ($k_{^3sens^*,TMP}$) were needed. There are reported values for $k_{^3sens^*,TMP}$ in the literature (Table 1); however, the value for 4-CBBP was determined at pH 10.2 with TMP being partially deprotonated. The $k_{^3sens^*,TMP}$ measured in this work for 3-MAP, 4-CBBP, and BP were 2.3-, 3.0-, and 1.3-fold faster, respectively, than those previously reported in the literature (Table 1, Figure 3, Text S1.3). Similar $k_{^3sens^*,TMP}$, near the diffusion-controlled limit, were expected based on the one-electron oxidation potential for TMP (1.22 V) being significantly lower than the reported one-electron reduction potentials of the three sensitizers, ranging from 1.64-1.95 V_{SHE} (Table 1).[12, 33, 35-37]

The $k_{^3sens^*,TMP}$ calculated in this work were used to calculate the bimolecular reaction rate constants between each ^{3}sens* and pesticide ($k_{^3sens^*}$) and to examine trends between $k_{^3sens^*}$ and sensitizer photochemical properties. There is, however, substantial uncertainty associated with this evaluation. More than one reduction potential value is reported for some sensitizers, and these values and the sensitizers' triplet energies were determined in either organic solvent/aqueous mixtures or in highly alkaline solutions.[12, 33, 35-37] Therefore, the true values of these properties may differ in pure water at neutral pH. There is also uncertainty when calculating $k_{^3sens^*,TMP}$ experimentally and the reported uncertainty may not fully capture the total uncertainty. For example, the spectral overlap between the molar absorptivity (ε_λ) of the sensitizer and the

irradiance of the UVA light source was limited to a small wavelength range (Figure S1.2), and measurements of ε_λ approached the detection limit of the UV-vis absorbance in this range. The variability in experimental values of ε_λ in this region was approximately ±35%, which was not propagated when calculating the sensitizers' rate of light absorption or subsequently calculating values of $k^{3}_{sens*,TMP}$.

Photoisomerization of Strobilurin Fungicides

Three of the pesticides – azoxystrobin, picoxystrobin, and trifloxystrobin – underwent photoisomerization in ^{3}sens* model systems, which was observed as biphasic degradation kinetics with a faster photoisomerization rate followed by a slower k^{3}_{sens*} (Figure 4, Figures S4.1-S4.2).[39] The initial photoisomerization rate was 2.6 to 10 times faster than the subsequent decay rate. Both bimolecular reaction rate constants are included in Figure 1 and Table S4.1 for completeness. Despite picoxystrobin and trifloxystrobin having four potential isomers, only one photoproduct peak appeared in the chromatogram during the initial photoisomerization phase for all three pesticides. This photoproduct was assumed to be an isomer based on similar absorbance spectra to the parent compound (Figure S4.3), the biphasic degradation kinetics observed, and the previous findings of azoxystrobin and trifloxystrobin photoisomerization during direct photolysis.[40-42] Although biphasic kinetics can help distinguish photoisomerization processes, it may not always be observed during photoisomerization.[43] For example, single-phase kinetics would be expected when experimental times are shorter than the time needed to reach photoisomerization equilibrium or if degradation occurs faster than photoisomerization.

Bimolecular Reaction Rate Constants between Triplet Excited States of Sensitizers (^{3}sens) and Pesticides*

Reactions with ^{3}sens* were observed for 89% (25 out of 28) of the pesticides (Figures 1C and S4.4-S4.8, Table S4.1). Of the 25 pesticides that reacted with ^{3}sens*, 16 contained functional groups previously identified as reactive with ^{3}CDOM*, including aniline substructures, amino-substituted aromatic heterocycles, and sulfur atoms (Figure S4.9).[11] This high degree of susceptibility to reactions with ^{3}sens* was expected based on the selection process used for candidate pesticides (i.e., pesticides suspected to be susceptible to indirect photodegradation). Consequently, reactions between ^{3}sens* or ^{3}CDOM* and a broader range of organic contaminants should be more selective than what results from this set of compounds would suggest.

Measured $k_{^3sens^*}$ spanned more than two orders of magnitude and the relative $k_{^3sens^*}$ among each ^{3}sens* differed across pesticides (Table S4.1, Figure 5). Nine pesticides (n=9/25) had $k_{^3sens^*}$ within a factor of 3 for all three sensitizers, including pesticides with both lower ($\approx 10^8$ M^{-1} s^{-1}) and higher reactivity ($\approx 10^9$ M^{-1} s^{-1}) towards ^{3}sens* (Figure 5A). Five more pesticides (n=5/25) had $k_{^3sens^*}$ within a factor of 5 for all three sensitizers (Figure 5B). Nevertheless, amongst these 14 pesticides with $k_{^3sens^*}$ within a factor of 3 or 5, whether $k_{^3sens^*}$ was fastest with ^{3}3-MAP*, ^{3}4-CBBP*, or ^{3}BP* varied. This precludes being able to correlate the measured $k_{^3sens^*}$ with a single sensitizer's photochemical properties.

Eight of the 11 remaining pesticides (n=8/25) had larger differences between $k_{^3sens^*}$ values, and the slowest or no reaction with ^{3}3-MAP* (Figure 5C). The slower reactivity with ^{3}3-MAP* could be due to either its lower one-electron reduction potential compared to 4-CBBP and BP or its π-π* triplet state configuration.[37] Both 4-CBBP and BP have n-π* triplet state configurations,

which has been shown to be more reactive than the π-π* configuration even at the same one-electron reduction potential.[33, 37, 44-46]

The remaining three pesticides (n=3/25) did not fit any of these patterns, including chlorothalonil (Figure 5D). Chlorothalonil is known to undergo energy transfer with ^{3}sens*, and its measured triplet energy (276 kJ mol^{-1}) is below that measured for all three sensitizers (Table 1).[21, 33, 35-37] Therefore, the faster $k_{^3sens^*}$ with ^{3}3-MAP* can be explained by 3-MAP's higher triplet energy. Overall, the observed differences amongst these pesticides illustrate that the ^{3}sens* reactions, even in simplified model systems, are not fully understood yet. Reactions with the complex mixture that constitutes CDOM should be expected to be even more complex.

Phenol Antioxidant Model Systems: Susceptibility to Back-Reactions

Previous research found that triplet-induced oxidation of aromatic amines was susceptible to back-reaction with the antioxidant moieties present in CDOM.[47-49] Therefore, decay rates with ^{3}CDOM* could be slower than expected based on $k_{^3sens^*}$. To evaluate the potential for back-reaction, phenol (10 μM) was used as a model antioxidant and 4-CBBP as the sensitizer. Observed degradation rates in the presence of phenol decreased for seven pesticides and increased for chlorothalonil (Figure S4.10-S4.11). Chlorothalonil is known to undergo photoreduction, which was enhanced by the antioxidant property of phenol.[21] The degradation rates of the remaining 20 pesticides investigated were similar with or without the addition of phenol (Figure S4.12).

Five of the seven pesticides that had slower degradation rates in the presence of phenol contained aromatic amine functional groups, whereas deprotonated prothioconazole and mesotrione did not (Figure S4.13). The thione in prothioconazole is a likely reaction site with ^{3}sens*.[11] However, the mechanisms for back-reactions for both deprotonated prothioconazole and

mesotrione are unclear and require further study. Additionally, not all pesticides with amines and/or aromatic amines underwent back-reactions – atrazine, pendimethalin, and protonated prothioconazole degradation rates were not affected by the addition of phenol (Figure S4.12).

Observed degradation rates of MCPA with ^{3}3-MAP* were significantly slower than with ^{3}4-CBBP* compared to other pesticides (Figure S4.4-S4.8). Therefore, antioxidant effects were tested with both sensitizers. Phenol addition slowed degradation by 24% with 4-CBBP and by 60% with 3-MAP (Figure S4.11). Previous findings showed that MCPA, excited by UVB irradiation, could react with phenol, but the presence of phenol at high concentrations (200-500 μM) decreased the direct photolysis rate by ≈40%.[50] Consequently, predicting $k_{^3CDOM^*}$ and the overall photodegradation rate may not be possible because CDOM can have variable photochemical properties and antioxidant content.

Steady-state concentrations of ^{3}sens* were quantified using TMP, a substituted phenol, as the probe compound. Control experiments without the probe (i.e., sensitizer and pesticide only) showed that TMP (10 μM) could also act as an antioxidant (Figures S4.10-S4.11). With TMP, observed degradation of cyprodinil, fluroxypyr, and pyrimethanil were slower by 39-84% compared to experiments without TMP (Figures S4.10). These three pesticides were also the most affected by back-reactions when phenol was added as a model antioxidant. In contrast, chlorothalonil degradation rates increased by 29-fold with ^{3}4-CBBP* in the presence of TMP (Figures S4.10). For MCPA, the observed degradation rate increased by 6-fold with ^{3}3-MAP* and 16% with ^{3}4-CBBP* in the presence of TMP (Figures S4.11). These observations for MCPA contrast with the slower degradation rate in the presence of phenol with both sensitizers. Consequently, for cyprodinil, fluroxypyr, pyrimethanil, chlorothalonil, and MCPA, the

degradation of both the pesticide and probe were measured in separate solutions to calculate $k_{^3sens^*}$ (Text S4.1, Figure S4.7).

Implications

Both 4-CBBP and BP have been proposed as reasonable surrogates for assessing ^{3}CDOM* reactivity.[14, 51] However, the reported photochemical properties of 3-MAP likely make it more representative for assessing susceptibility to reaction with ^{3}CDOM*. Using 3-MAP is also more conservative and should minimize overestimating contributions of ^{3}CDOM* to environmental degradation. Nevertheless, 4-CBBP and BP remain valuable for investigating reaction mechanisms with triplet excited species, especially BP which typically had faster reaction rates with the pesticides investigated and has the benefit of being a well-studied photochemical sensitizer since the 1970s. As for the probe compound, TMP has been considered suitable for quantifying ^{3}CDOM* (or ^{3}sens*) in experiments due to its high reactivity, slow direct photolysis rate under sunlight, and lack of inhibition from antioxidants.[27] However, its own antioxidant properties have been largely overlooked. For compounds that react with ^{3}sens*, control experiments without TMP are needed.

No clear pattern in $k_{^3sens^*}$ was observed between the different pesticides and model sensitizers, indicating that more study of ^{3}sens* reaction mechanisms and photochemical properties in aqueous systems is needed. Nevertheless, results from these ^{3}sens* model systems are still expected to be more interpretable than ^{3}CDOM* experiments with or without the use of quenchers (Figure S2.2B, Table S4.1). For example, a previous study using CDOM and quenchers found that photodegradation of propiconazole would be predominantly through reaction with $^1O_2$ and ^{3}CDOM*, but propiconazole did not degrade with either PPRI in these model systems.[52]

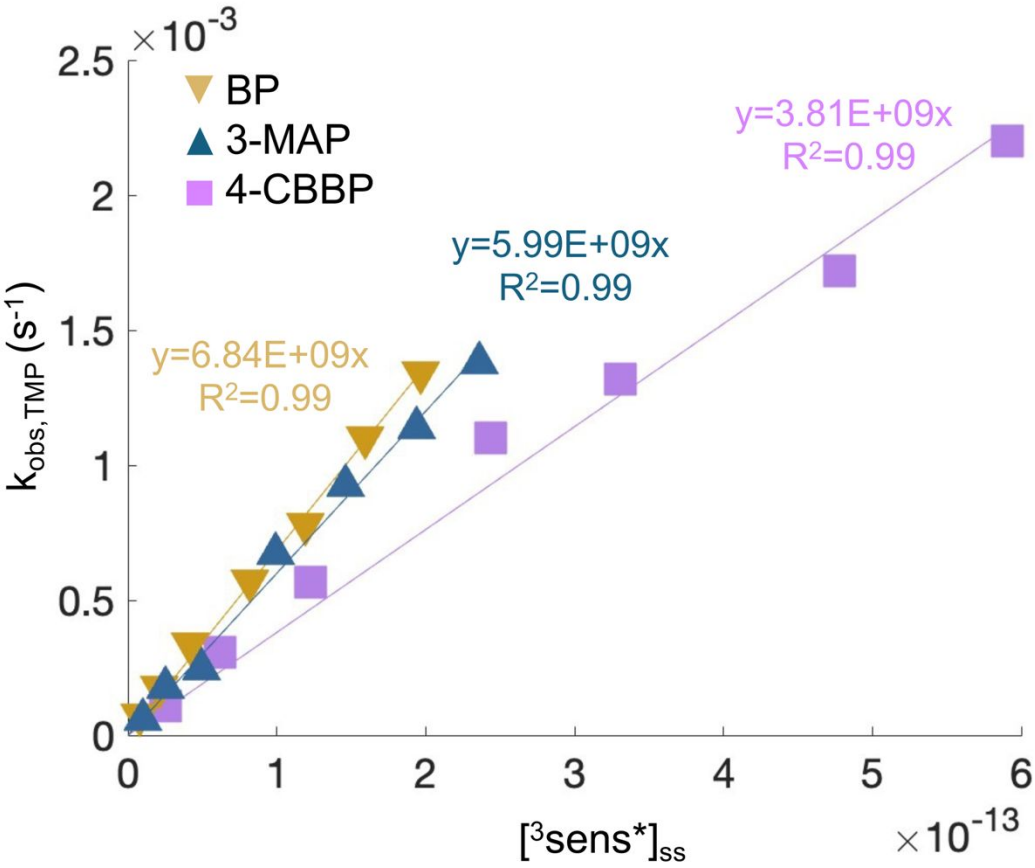

Figure 3. Observed degradation rates of the probe compound (TMP) as a function of the calculated steady-state concentrations of the triplet excited states of each model sensitizer ($[^3sens^*]_{ss}$; Table S1.4 and Text S1.3). The slopes of the linear regression are the bimolecular reaction rate constants between $^3sens^*$ and TMP and the coefficient of determination (R^2) is also provided.

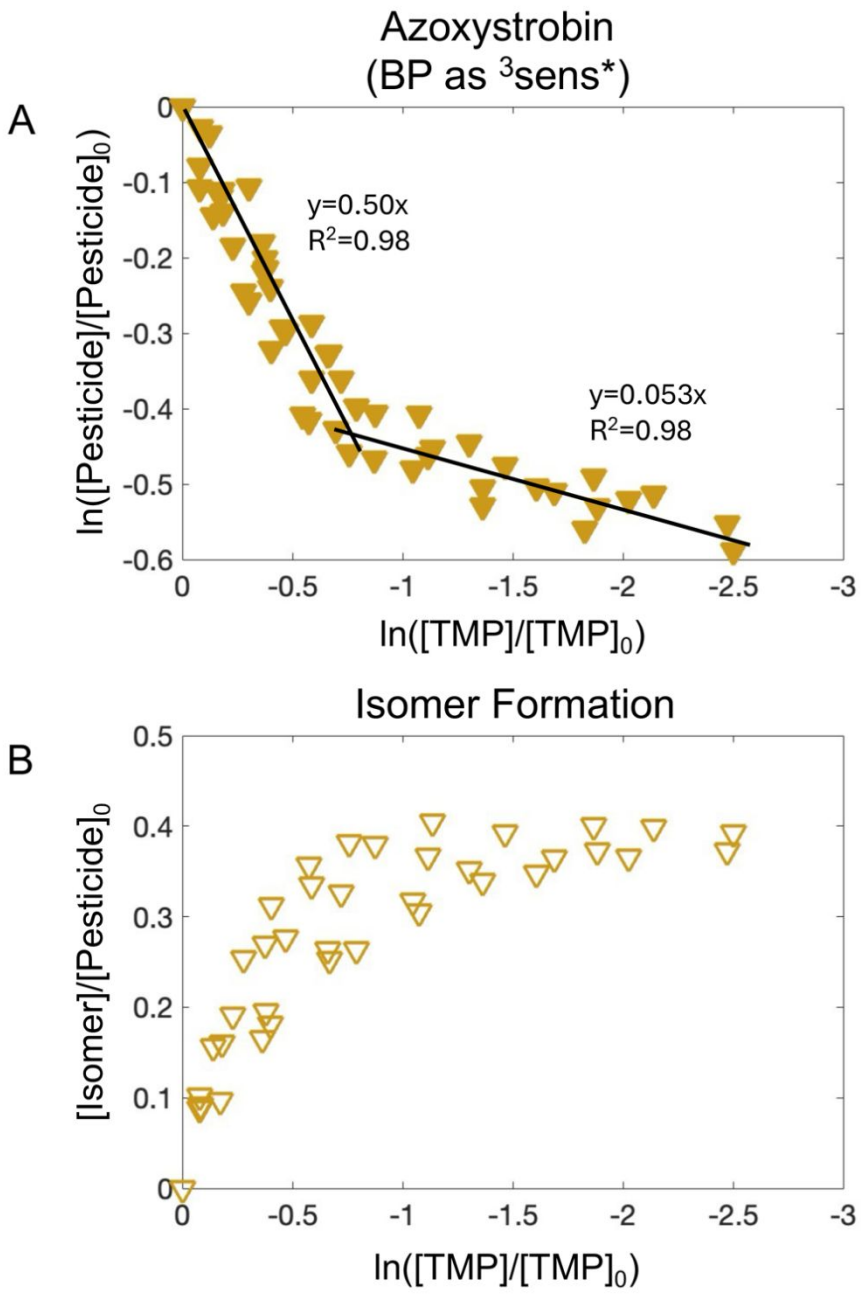

460

461 Figure 4. Observed degradation (A) and formation of the photoproduct, presumed to be an isomer,
462 (B) of azoxystrobin. The molar absorptivities of parent compound and its isomer were assumed to
463 be the same at the wavelength used for quantification (Table S1.3) in order to calculate isomer
464 formation rates. The slopes and the coefficient of determination (R^2) of azoxystrobin's degradation
465 are provided.

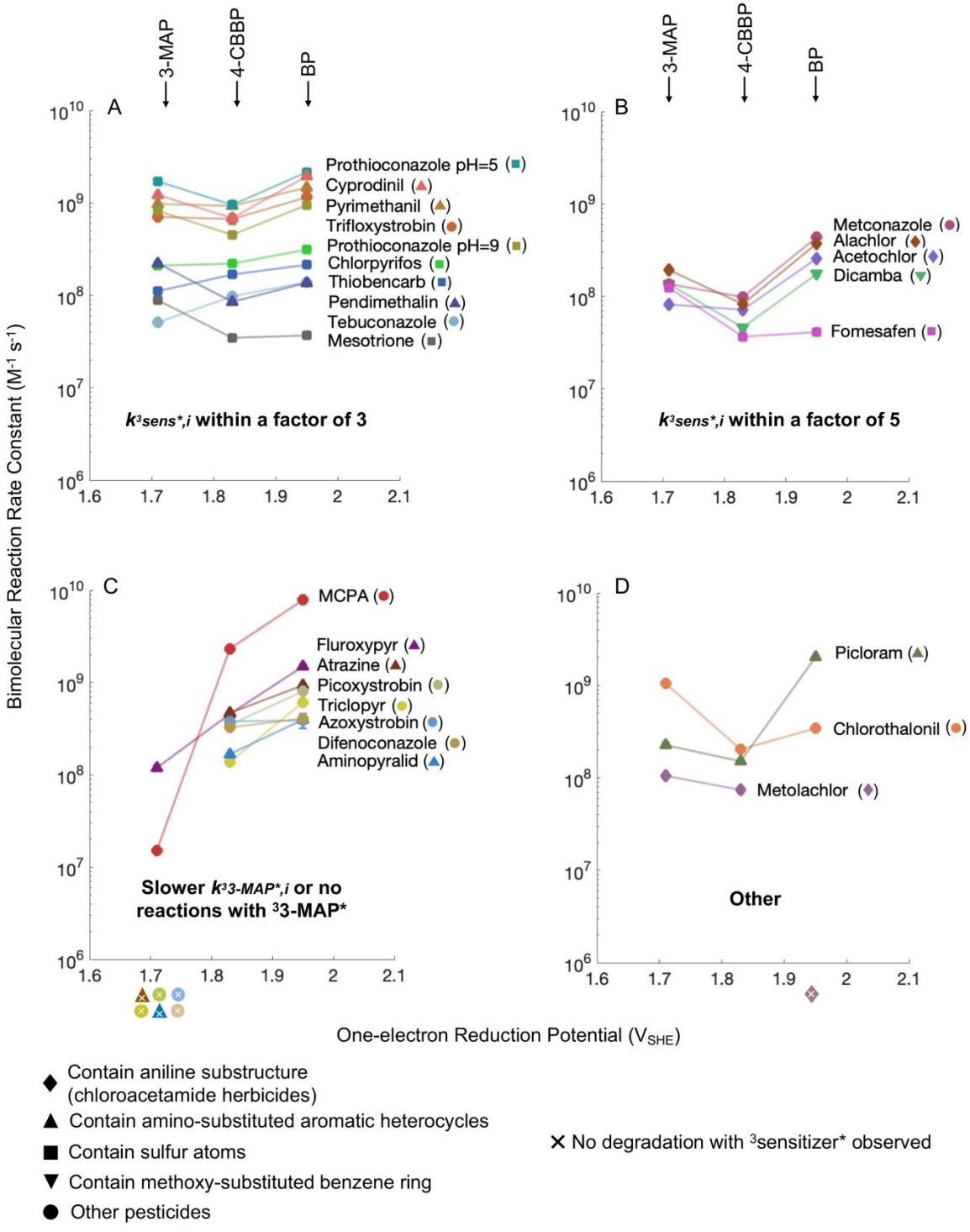
A
3-MAP
4-CBBP
BP
Prothioconazole pH=5
Cyprodinil
Pyrimethanil
Trifloxystrobin
Prothioconazole pH=9
Chlorpyrifos
Thiobencarb
Pendimethalin
Tebuconazole
Mesotrione
k³sens*,i within a factor of 3
B
Metconazole
Alachlor
Acetochlor
Dicamba
Fomesafen
k³sens*,i within a factor of 5
C
MCPA
Fluroxypyr
Atrazine
Picoxystrobin
Triclopyr
Azoxystrobin
Difenoconazole
Aminopyralid
Slower k³3-MAP*,i or no reactions with ³3-MAP*
D
Picloram
Chlorothalonil
Metolachlor
Other
Bimolecular Reaction Rate Constant (M⁻¹ s⁻¹)
One-electron Reduction Potential (V_SHE)
Contain aniline substructure (chloroacetamide herbicides)
Contain amino-substituted aromatic heterocycles
Contain sulfur atoms
Contain methoxy-substituted benzene ring
Other pesticides
No degradation with ³sensitizer* observed

466

Figure 5. Bimolecular reaction rate constants between ^{3}sens* and the pesticide ($k_{^3sens^*}$, Table S4.1) as a function of the sensitizers' one-electron reduction potentials reported in Table 1. Pesticides were grouped according to their relative $k_{^3sens^*}$ patterns. In panel (A), the $k_{^3sens^*}$ measured with 4-CBBP, BP, and 3-MAP were within a factor of 3, in (B) the $k_{^3sens^*}$ were within a factor of 5, in (C) $k_{^3sens^*}$ had larger differences and were slower or unreactive with ^{3}3-MAP*, and in (D) the pesticides did not follow any of the trends observed in (A-C). The different symbols chosen for plotting $k_{^3sens^*}$ values of each pesticide were based on common functional groups previously identified as reaction sites for ^{3}CDOM* oxidation (Figure S4.9).[11] The cross symbol (×) indicates no degradation with that ^{3}sens* was observed. The highest one-electron reduction potentials reported for the sensitizers in Table 1 were selected for plotting the data.

ENVIRONMENTAL IMPLICATIONS AND NEXT STEPS

In this work, at least two model systems were used to quantify reaction rates between organic contaminants and various PPRI (•OH, $^1O_2$, and three ^{3}CDOM* proxies). The results showed that reactivity with •OH is the least selective and will likely have the fastest k_{PPRI} for many anthropogenic organic contaminants. However, the •OH steady-state concentration present in natural waters is orders of magnitude lower than that of $^1O_2$ and ^{3}CDOM*. Conversely, reactivity with $^1O_2$ was the most selective and typically had slower k_{PPRI}. Furthermore, all 10 pesticides that reacted with $^1O_2$ also degraded in ^{3}sens* model systems, with $k_{^3sens^*}$ found to be 3.6 to 9,200 times faster than $k_{^1O_2}$ (Tables S3.1 and S4.1). Consequently, in sunlit waters where the steady-state concentrations of $^1O_2$ and ^{3}CDOM* are expected to be approximately equal, reactions with $^1O_2$ may be significantly less important than those with ^{3}CDOM* for pesticides that are susceptible to both reaction pathways.[11]

To evaluate the environmental relevance of reactions with ^{3}CDOM*, the bimolecular reaction rate constant between ^{3}CDOM* and the pesticide ($k_{^3CDOM^*}$) required to achieve a $t_{1/2}$=30 days in sunlit waters was calculated, again assuming the steady-state concentration of ^{3}CDOM* and $^1O_2$ are approximately equal.[11] The $^1O_2$ steady-state concentration was previously modeled to be 1.9×10^{-14} M for near-surface conditions, which suggests pesticides with a $k_{^3CDOM^*} \geq 1.41\times10^7$ M^{-1} s^{-1} would have a calculated $t_{1/2} \leq$30 days.[11, 53] The slowest $k_{^3sens^*}$ measured in this work was 1.51×10^7 M^{-1} s^{-1} (Table S4.1). While these findings suggest that reactions of these pesticides with ^{3}CDOM* could be an environmentally relevant degradation pathway, it should be noted that the one-electron reduction potentials and triplet energies of the ^{3}sens* are at the high end of the range of estimates for ^{3}CDOM* (1.36-1.95 V_{SHE} and 180-320 kJ mol^{-1}).[11] Thus, pesticide degradation by ^{3}CDOM* could be substantially slower because of this, as well as potential back-reactions due to the antioxidant moieties naturally present in CDOM.

While this work showed the value of model systems for studying indirect photodegradation reactions, it also highlighted that more work is needed to fully understand the PPRI created and the potential reaction pathways of anthropogenic pollutants. First, at least one pesticide showed unexpected reactivity in each model system and control experiment. This shows that, in addition to the dark controls and direct photolysis controls that are typically conducted, control experiments that exclude the probe compound are also necessary. Furthermore, using the KSIE was needed to quantify the relative contributions of reactions with $^1O_2$ and ^{3}sens* because the production of these PPRI is inextricably linked.

Several pesticides in this work had calculated k_{PPRI} that suggests there are additional, unidentified PPRI produced in the model systems and/or possible unidentified reaction pathways for that pesticide. Of note are (1) the $k_{^{\bullet}OH}$ values above the diffusion-controlled limit, (2) the

substantial differences in reactivity between similar molecules (e.g., protonated vs. deprotonated prothioconazole and cyprodinil vs. pyrimethanil), and (3) the inconsistent reactivity pattern for the three ^{3}CDOM* proxies evaluated. The observed antioxidant effects of the commonly used ^{3}CDOM* probe, TMP, also indicates that a systematic comparison of probe compounds would be beneficial for the photochemistry community. Possible objectives of such a study could be to identify a more selective ^{3}CDOM* probe that would capture only the higher energy fraction of the ^{3}CDOM* or a set of probes that could be used to better understand and quantify the role of antioxidants during indirect photodegradation.

Despite these identified needs for further study, model systems still proved to be a promising step forward in increasing our mechanistic understanding of environmental degradation pathways and ultimately to developing predictive models of environmental fate. Following the current US EPA guidelines does not produce any k_{PPRI}, only an apparent pseudo-first order reaction rate that is applicable to only the specific water composition used in that experiment. Therefore, the US EPA guidelines should be updated, and model systems should become commonly used when evaluating the fate of pesticides during their registration.

ACKNOWLEDGEMENTS

This research was supported by the United States Department of Agriculture (USDA NIFA grant number 2022-67020-37182). The authors gratefully acknowledge Dr. Miguel Modestino and Dr. Jonathan Challis for valuable discussions.

CONFLICTS OF INTEREST

There are no conflicts to declare.

REFERENCES

1. J. N. Apell, N. C. Pflug and K. McNeill, Photodegradation of Fludioxonil and Other Pyrroles: The Importance of Indirect Photodegradation for Understanding Environmental Fate and Photoproduct Formation, *Environ Sci Technol*, 2019, **53**, 11240-11250.
2. C. K. Remucal, The role of indirect photochemical degradation in the environmental fate of pesticides: a review, *Environ Sci Process Impacts*, 2014, **16**, 628-653.
3. D. E. Latch, B. Stender, J. L. Packer, W. A. Arnold and K. McNeill, Photochemical Fate of Pharmaceuticals in the Environment: Cimetidine and Ranitidine, *Environ Sci Technol*, 2003, **37**, 3342-3350.
4. J. L. Packer, J. J. Werner, D. E. Latch, K. McNeill and W. A. Arnold, Photochemical fate of pharmaceuticals in the environment: Naproxen, diclofenac, clofibric acid, and ibuprofen, *Aquatic Sciences - Research Across Boundaries*, 2003, **65**, 342-351.
5. U. S. E. P. Agency, Fate, Transport and Transformation Test Guidelines: OPPTS 835.5270 Indirect Photolysis Screening Test.*Journal*, 1998.
6. A. Fairbrother, D. Muir, K. R. Solomon, G. T. Ankley, M. A. Rudd, A. B. A. Boxall, J. N. Apell, K. L. Armbrust, B. J. Blalock, S. R. Bowman, L. M. Campbell, G. P. Cobb, K. A. Connors, D. A. Dreier, M. S. Evans, C. J. Henry, R. A. Hoke, M. Houde, S. J. Klaine, R. D. Klaper, S. A. Kullik, R. P. Lanno, C. Meyer, M. A. Ottinger, E. Oziolor, E. J. Petersen, H. C. Poynton, P. J. Rice, G. Rodriguez-Fuentes, A. Samel, J. R. Shaw, J. A. Steevens, T. A. Verslycke, D. E. Vidal-Dorsch, S. M. Weir, P. Wilson and B. W. Brooks, Toward Sustainable Environmental Quality: Priority Research Questions for North America, *Environ Toxicol Chem*, 2019, **38**, 1606-1624.

7. A. E. Herner and B. Acock, in *Encyclopedia of Agrochemicals*, DOI: https://doi.org/10.1002/047126363X.agr237.

8. P. Calza, D. Vione, A. Novelli, E. Pelizzetti and C. Minero, The role of nitrite and nitrate ions as photosensitizers in the phototransformation of phenolic compounds in seawater, *Sci Total Environ*, 2012, **439**, 67-75.

9. K. Cheng, H. Li, J. R. Laszakovits, C. M. Sharpless, F. Rosario-Ortiz and G. McKay, Probing the Photochemical Formation of Hydroxyl Radical from Dissolved Organic Matter: Insights into the H(2)O(2)-Dependent Pathway, *Environ Sci Technol*, 2025, **59**, 2245-2256.

10. R. Ossola, M. Schmitt, P. R. Erickson and K. McNeill, Furan Carboxamides as Model Compounds To Study the Competition between Two Modes of Indirect Photochemistry, *Environ Sci Technol*, 2019, **53**, 9594-9603.

11. K. McNeill and S. Canonica, Triplet state dissolved organic matter in aquatic photochemistry: reaction mechanisms, substrate scope, and photophysical properties, *Environ Sci Process Impacts*, 2016, **18**, 1381-1399.

12. S. Canonica, B. Hellrung, P. Muller and J. Wirz, Aqueous Oxidation of Phenylurea Herbicides by Triplet Aromatic Ketones, *Environ Sci Technol*, 2006, **40**, 6636-6641.

13. M. Minella, L. Rapa, L. Carena, M. Pazzi, V. Maurino, C. Minero, M. Brigante and D. Vione, An experimental methodology to measure the reaction rate constants of processes sensitised by the triplet state of 4-carboxybenzophenone as a proxy of the triplet states of chromophoric dissolved organic matter, under steady-state irradiation conditions, *Environ Sci Process Impacts*, 2018, **20**, 1007-1019.

14. L. Carena, C. G. Puscasu, S. Comis, M. Sarakha and D. Vione, Environmental photodegradation of emerging contaminants: A re-examination of the importance of triplet-sensitised processes, based on the use of 4-carboxybenzophenone as proxy for the chromophoric dissolved organic matter, *Chemosphere*, 2019, **237**, 124476.

15. C. A. Davis, K. McNeill and E. M. Janssen, Non-Singlet Oxygen Kinetic Solvent Isotope Effects in Aquatic Photochemistry, *Environ Sci Technol*, 2018, **52**, 9908-9916.

16. L. de Brito Anton, A. I. Silverman and J. N. Apell, Determining wavelength-dependent quantum yields of photodegradation: importance of experimental setup and reference values for actinometers, *Environ Sci Process Impacts*, 2024, **26**, 1052-1063.

17. G. V. Buxton, C. L. Greenstock, W. P. Helman and A. B. Ross, Critical Review of rate constants for reactions of hydrated electrons, hydrogen atoms and hydroxyl radicals (·OH/·O− in Aqueous Solution, *Journal of Physical and Chemical Reference Data*, 1988, **17**, 513-886.

18. E. Appiani, R. Ossola, D. E. Latch, P. R. Erickson and K. McNeill, Aqueous singlet oxygen reaction kinetics of furfuryl alcohol: effect of temperature, pH, and salt content, *Environ Sci Process Impacts*, 2017, **19**, 507-516.

19. P. Pakulski and D. Pinkowicz, 1,2,5-Thiadiazole 1,1-dioxides and Their Radical Anions: Structure, Properties, Reactivity, and Potential Use in the Construction of Functional Molecular Materials, *Molecules*, 2021, **26**.

20. U. S. E. P. Agency, *Pesticide Fact Sheet: Prothioconazole*, 2007.

21. J. Porras, J. J. Fernandez, R. A. Torres-Palma and C. Richard, Humic substances enhance chlorothalonil phototransformation via photoreduction and energy transfer, *Environ Sci Technol*, 2014, **48**, 2218-2225.

22. J.-W. Park, S.-E. Lee, I.-K. Rhee and J.-E. Kim, Transformation of the Fungicide Chlorothalonil by Fenton Reagent, *J. Agric. Food Chem.*, 2002, **50**, 7570-7575.

23. R. C. Scholes, C. Prasse and D. L. Sedlak, The Role of Reactive Nitrogen Species in Sensitized Photolysis of Wastewater-Derived Trace Organic Contaminants, *Environ Sci Technol*, 2019, **53**, 6483-6491.

24. D. Vione, M. Minella, V. Maurino and C. Minero, Indirect photochemistry in sunlit surface waters: photoinduced production of reactive transient species, *Chemistry*, 2014, **20**, 10590-10606.

25. V. V. Goncharuk, N. M. Soboleva and A. A. Nosonovich, Photooxidative destruction of organic compounds by hydrogen peroxide in water, *Journal of Water Chemistry and Technology*, 2010, **32**, 17-32.

26. S. Xie, C. Tang, H. Shi and G. Zhao, Highly efficient photoelectrochemical removal of atrazine and the mechanism investigation: Bias potential effect and reactive species, *J Hazard Mater*, 2021, **415**, 125681.

27. F. L. Rosario-Ortiz and S. Canonica, Probe Compounds to Assess the Photochemical Activity of Dissolved Organic Matter, *Environ Sci Technol*, 2016, **50**, 12532-12547.

28. C. Minero, S. Chiron, G. Falletti, V. Maurino, E. Pelizzetti, R. Ajassa, M. E. Carlotti and D. Vione, Photochemincal processes involving nitrite in surface water samples, *Aquatic Sciences*, 2007, **69**, 71-85.

29. Y. Huang, M. Kong, D. Westerman, E. G. Xu, S. Coffin, K. H. Cochran, Y. Liu, S. D. Richardson, D. Schlenk and D. D. Dionysiou, Effects of HCO(3)(-) on Degradation of Toxic Contaminants of Emerging Concern by UV/NO(3)(), *Environ Sci Technol*, 2018, **52**, 12697-12707.

30. J. Zhang, L. Zheng, F. Wang, C. Chen, H. Wu, S. A. K. Leghari and M. Long, The critical role of furfural alcohol in photocatalytic H2O2 production on TiO2, *Applied Catalysis B: Environmental*, 2020, **269**.

31. E. L. Clennan and A. Pace, Advances in singlet oxygen chemistry, *Tetrahedron*, 2005, **61**, 6665-6691.

32. M. V. George and V. Bhat, Photooxygenations of Nitrogen Heterocycles, *Chem Rev.*, 1979, **79**, 447-478.

33. J. K. Hurley, H. Linschitz and A. Treinin, Interaction of Halide and Pseudohalide Ions with Triplet Benzophenone-4-carboxylate: Kinetics and Radical Yields, *J. Phys. Chem.*, 1988, **92**, 5151-5159.

34. C. Chu, P. R. Erickson, R. A. Lundeen, D. Stamatelatos, P. J. Alaimo, D. E. Latch and K. McNeill, Photochemical and Nonphotochemical Transformations of Cysteine with Dissolved Organic Matter, *Environ Sci Technol*, 2016, **50**, 6363-6373.

35. P. B. Merkel and J. P. Dinnocenzo, Thermodynamic energies of donor and acceptor triplet states, *Journal of Photochemistry and Photobiology A: Chemistry*, 2008, **193**, 110-121.

36. A. J. G. Barwise, A. A. Gorman, R. L. Leyland, P. G. Smith and M. A. J. Rodgers, A pulse radiolysis study of the quenching of aromatic carbonyl triplets by norbornadienes and quadricyclenes. The mechanism of interconversion, *Environ Sci Technol*, 1978, **100**.

37. H. Shizuka and H. Obuchi, Anion-Induced Triplet Quenching of Aromatic Ketones by Nanosecond Laser Photolysis, 1982, **86**, 1297-1302.

38. S. Canonica, B. Hellrung and J. Wirz, Oxidation of Phenols by Triplet Aromatic Ketones in Aqueous Solution, *J. Phys. Chem. A*, 2000, **104**, 1226-1232.

39. C. Dugave and L. Demange, Cis-Trans Isomerization of Organic Molecules and Biomolecules: Implications and Applications, *Chem Rev.*, 2003, **103**, 2475-2532.

40. A. Boudina, C. Emmelin, A. Baaliouamer, O. Paisse and J. M. Chovelon, Photochemical transformation of azoxystrobin in aqueous solutions, *Chemosphere*, 2007, **68**, 1280-1288.

41. J. Chastain, A. ter Halle, P. de Sainte Claire, G. Voyard, M. Traikia and C. Richard, Phototransformation of azoxystrobin fungicide in organic solvents. Photoisomerization vs. photodegradation, *Photochem Photobiol Sci*, 2013, **12**, 2076-2083.

42. K. Banerjee, A. P. Ligon and M. Spiteller, Photoisomerization kinetics of trifloxystrobin, *Anal Bioanal Chem*, 2005, **382**, 1527-1533.

43. J. Lin, J. N. Apell, K. McNeill, M. Emberger, V. Ciraulo and S. Gimeno, A streamlined workflow to study direct photodegradation kinetic and transformation products for persistence assessment of a fragrance ingredient in natural waters, *Environ Sci Process Impacts*, 2019, **21**, 1713-1721.

44. S. G. Cohen, G. A. Davis and W. D. K. Clark, Photoreduction of pi-pi* Triplets by Amines, 2-Naphthaldehyde, and 2-Acetonaphthone, *Journal of the American Chemical Society*, 1972, **94**.

45. P. J. Wagner, R. J. Truman, A. E. Puchalski and R. Wake, Extent of Charge Transfer in the Photoreduction of Phenyl Ketones by Alkylbenzenes, *Journal of the American Chemical Society*, 1986, **108**, 7727-7738.

46. J. Khan and S. G. Cohen, Photoreduction of pi-pi* and n-pi* Triplet Carbonyls by Amines: 2-Naphthaldehyde, 2-Acetonaphthone, p-Aminobenzophenone, and p-Cyanobenzophenone, *J Org Chem*, 1991, **56**, 938-943.

47. S. Canonica and H. U. Laubscher, Inhibitory effect of dissolved organic matter on triplet-induced oxidation of aquatic contaminants, *Photochem Photobiol Sci*, 2008, **7**, 547-551.

48. J. Wenk, U. von Gunten and S. Canonica, Effect of dissolved organic matter on the transformation of contaminants induced by excited triplet states and the hydroxyl radical, *Environ Sci Technol*, 2011, **45**, 1334-1340.

49. J. Wenk and S. Canonica, Phenolic antioxidants inhibit the triplet-induced transformation of anilines and sulfonamide antibiotics in aqueous solution, *Environ Sci Technol*, 2012, **46**, 5455-5462.

50. D. Vione, S. Khanra, R. Das, C. Minero, V. Maurino, M. Brigante and G. Mailhot, Effect of dissolved organic compounds on the photodegradation of the herbicide MCPA in aqueous solution, *Water Res*, 2010, **44**, 6053-6062.

51. W. A. Arnold, One electron oxidation potential as a predictor of rate constants of N-containing compounds with carbonate radical and triplet excited state organic matter, *Environ Sci Process Impacts*, 2014, **16**, 832-838.

52. T. Zeng and W. A. Arnold, Pesticide photolysis in prairie potholes: probing photosensitized processes, *Environ Sci Technol*, 2013, **47**, 6735-6745.

53. S. B. Partanen, J. N. Apell, J. Lin and K. McNeill, Factors affecting the mixed-layer concentrations of singlet oxygen in sunlit lakes, *Environ Sci Process Impacts*, 2021, **23**, 1130-1145.

DATA AVAILABILITY STATEMENT

The data supporting this manuscript are available in the Supplementary Information section of this manuscript. All relevant external data sources are cited in the main text and the Supplementary Information.